online data

Antimicrobial activity of omwaprin, a new member of the waprin family of snake venom proteins

Dileep G. NAIR*, Bryan G. FRY*†[1], Paul ALEWOOD†, Prakash P. KUMAR*‡[2] and R. Manjunatha KINI*§[2]

*Department of Biological Sciences, Faculty of Science, National University of Singapore, Singapore 117543, †Institute for Molecular Bioscience, University of Queensland, Brisbane, Australia 4072, ‡Temasek Life Sciences Laboratory, 1 Research Link, National University of Singapore, Singapore 117604, and §Department of Biochemistry and Molecular Biophysics, Medical College of Virginia, Virginia Commonwealth University, Richmond, VA 23298, U.S.A.

We have isolated and characterized omwaprin, a 50-amino-acid cationic protein from the venom of inland taipan (*Oxyuranus microlepidotus*). It is a new member of the waprin family of snake venom proteins. A synthetic gene was designed and constructed for expressing the recombinant protein in *Escherichia coli*. Recombinant omwaprin was used for carrying out functional analyses. The protein is non-toxic to Swiss albino mice at doses of up to 10 mg/kg when administered intraperitoneally. However, it shows selective and dose-dependant antibacterial activity against Gram-positive bacteria. The minimum inhibitory doses were in the range 2–10 μg for selected species of bacteria in radial diffusion assays. The antibacterial activity is salt-tolerant up to 350 mM NaCl. However, omwaprin lost its antibacterial activity upon reduction and alkylation of its cysteine residues, or upon deletion of six N-terminal amino acid residues, four of which are positively charged. These observations indicate that the three-dimensional structure constrained by four disulfide bonds and the N-terminal residues are essential for its activity. The mechanism of action is via membrane disruption, as shown by scanning electron microscopy. Importantly, omwaprin lacks haemolytic activity on human erythrocytes. This demonstrates the specificity of omwaprin for bacterial membranes. Unlike other reported WAP (whey acidic protein) domain-containing antibacterial proteins, including elafin, EPPIN (epididymal proteinase inhibitor), SWAM1 and SWAM2 [single WAP (whey acidic protein) motif proteins 1 and 2] and SLPI (secretory leucocyte proteinase inhibitor), omwaprin shows species-specific activity on the Gram-positive bacteria tested.

Key words: antibacterial protein, antimicrobial protein, inland taipan (*Oxyuranus microlepidotus*), omwaprin, snake venom, WAP domain (whey acidic protein domain).

INTRODUCTION

Snake venoms are complex mixtures of pharmacologically active proteins and polypeptides. The snake venom proteins are of biological interest because of their diverse and selective pharmacological and physiological effects through their interaction with various molecular targets. These proteins are prototypes for: (i) therapeutic agents (Captopril, an antihypertensive drug, is a classic example that was designed based on the peptide inhibitor of angiotensin-converting enzyme from *Bothrops jararaca* venom [1]); (ii) pharmacological probes for the diagnosis of several diseases (thrombin-like enzymes from snake venom are used for fibrinogen and fibrinogen-breakdown product assays as well as detecting dysfibrinogenaemias [2]. Also, snake venom C-type lectins are routinely used to study platelet glycoprotein receptors [3]); and (iii) research tools to decipher physiological and pathological processes [4]. Peptide neurotoxins from snake venoms are used for the identification and characterization of membrane ion channels and receptors in vertebrate cells, including human neurons [5]. It has also been demonstrated that snake venom metalloproteinases and peptide neurotoxins can be used to study myoblast fusion and fertilization, and matrix metalloproteinase–cell interactions can be used for characterizing human cancers and small-cell carcinoma [4]. All of these studies demonstrate the significance of snake venom proteins as valuable tools for basic research, disease diagnosis and drug development. However, most snake venoms remain poorly characterized despite being a rich source of biologically active proteins with therapeutic potential. Hence, further studies are essential to identify and characterize novel venom proteins which can be used as leads or structural templates for developing new therapeutic agents.

Snake venom proteins and polypeptides are classified into superfamilies of enzymes and non-enzymatic proteins. The members of each superfamily show similarity in their primary, secondary and tertiary structures, but, at times, their biological functions are distinct [6]. Among non-enzymatic proteins, superfamilies of three-finger toxins [7], serine proteinase inhibitors [8], C-type lectin-related proteins [9], atrial natriuretic peptides [10] and nerve growth factors [11] are well characterized.

New protein families continue to be described from snake venoms. For example, new families of snake venom proteins called waprins and vespryns were described recently from studies in our laboratory [12,13]. Waprins show structural similarity to WAPs (whey acidic proteins) [12]. The WAP domain generally consists of 50 amino acid residues, with eight conserved cysteine residues forming four disulfide bonds. Even though the cysteine residues are conserved, the inter-cysteine segments are

Abbreviations used: CDAP, 1-cyano-4-dimethylaminopyridinium; cfu, colony-forming units; CN-induced cleavage, cleavage by aqueous ammonia at the N-terminus of cyanylated cysteine residues; EPPIN, epididymal proteinase inhibitor; ESI, electrospray ionization; GdmCl, guanidinium chloride; HE2, human epididymis 2; IPTG, isopropyl β-D-thiogalactoside; itz, iminothiazolidine; LB, Luria–Bertani; LC, liquid chromatography; MALDI–TOF, matrix-assisted laser-desorption ionization–time-of-flight; MID, minimum inhibitory dose; PLA_2, phospholipase A_2; *p*NA, *p*-nitroanilide; RP, reverse-phase; SEM, scanning electron microscopy; SLPI, secretory leucocyte proteinase inhibitor; SWAM, single WAP (whey acidic protein) motif protein; TCEP, tris-(2-carboxyethyl)phosphine; TFA, trifluoroacetic acid; WAP, whey acidic protein.

[1] Present address: Australian Venom Research Unit, Level 8, School of Medicine, University of Melbourne, Parkville, Victoria 3010, Australia.

[2] Correspondence may be addressed to either of these authors (email dbskumar@nus.edu.sg or dbskinim@nus.edu.sg).

The protein sequence data reported have been submitted to the Swiss-Prot Database under the accession number P83952.

entirely different among the WAP family members. Moreover, the WAP domain is found in proteins with divergent functions, including SPAI (Na^+,K^+-ATPase inhibitor), which inhibits Na^+-K^+ ATPase [14], elafin and SLPI (secretory leucocyte proteinase inhibitor), which are proteinase inhibitors with potent antimicrobial activity [15,16], ps20 with growth-inhibitory activity [17], and SWAM1 and SWAM2 (single WAP motif proteins 1 and 2), which are antibacterial proteins [18]. Many of the reported WAP domain proteins are involved in the innate immune system. Nawaprin, the first WAP domain protein from snake venom, has been structurally well characterized using NMR techniques [12]. The three-dimensional structure of nawaprin shows significant similarity to that of elafin, with a flat disc-like shape, characterized by a spiral backbone configuration that forms outer and inner circular segments [12]. The biological function(s) of nawaprin has yet to be identified.

In the present paper, we report the identification, purification and functional characterization of a new member of waprin family, omwaprin from the venom of inland taipan (*Oxyuranus microlepidotus*). Omwaprin is cationic under physiological conditions and shows selective antibacterial activity against Gram-positive bacteria. Our results show that this antibacterial activity is structure-dependent, salt–tolerant and specifically targets bacterial membranes. The potential of this novel antibacterial protein as a research tool and as a prototype for the development of therapeutic agents will be highlighted.

EXPERIMENTAL

Bacterial strains

Escherichia coli BL21-CodonPlus(DE3)-RIL cells (Novagen) were used for protein expression, and the strains used for antibacterial assays included the Gram-positive *Bacillus megaterium* (IAM 13418 T), *Bacillus thuringiensis* (WS 2617), *Streptomyces clavuligerus* (NRRL 3585), *Staphylococcus warneri* (AJ 276810), *Staphylococcus aureus* (ATCC 25923) and two Gram-negative species, *E. coli* (BL 21) and *Agrobacterium tumefaciens* (GV 3101). Bacteria were grown overnight in LB (Luria–Bertani) medium with continuous shaking at different temperature optima for each strain. The bacterial cultures were stored at $-80\,^{\circ}C$ in 25 % (w/v) glycerol.

Animals

Adult male Swiss albino mice weighing 18–22 g were used for the animal experiments. The mice were maintained on commercial standard pellet diet and tap water *ad libitum*. All of the animal experiments were carried out according to guidelines set by the Laboratory Animal Holding Center of the National University of Singapore [19].

Identification and isolation of omwaprin

Freeze-dried venom of *O. microlepidotus* (Venom Supplies Pty) was diluted to a concentration of 10 mg/ml, centrifuged at 1500 ***g*** for 2 h in Centricon 50 centrifuge filters (50 kDa cut-off) (Millipore), and the filtrate was centrifuge-filtered again using Centricon 10 tubes (10 kDa cut-off). The filtrates from this step were freeze-dried and stored until needed for LC (liquid chromatography)–MS analysis. Online LC–MS analysis of venoms was performed on a Vydac C_{18} analytical column [2.1 mm × 35 mm, 5 μm particle size, 300 Å (1 Å = 0.1 nm) pore size] with solvent A [0.05 % (v/v) TFA (trifluoroacetic acid)] and solvent B [90 % (v/v) acetonitrile in 0.045 % TFA] (Sigma) at a turbospray flow rate of 130 μl/min. The solvent delivery and gradient formation were achieved using an Applied Biosystems 140 B solvent-delivery system. The variable gradient was 0–20 % in the first 2 min and then 20–45 % over the next 12 min, followed by 45–80 % over the next 1 min. ESI (electrospray ionization) mass spectra were acquired on a PE-SCIEX triple-quadrupole mass spectrometer that was equipped with an Ionspray atmospheric pressure ionization source. The samples were used directly for mass analysis. Orifice potential was kept at 80 V. Nitrogen was used as a nebulizer and curtain gas. Data were acquired over the ion range 400–2100 *m*/*z* with a step size of 0.2 Da. Data processing was performed with the aid of the software package Biomultiview (PerkinElmer Sciex).

Characterization of omwaprin

A Vydac Preparative C_{18} column (4.9 mm × 250 mm, 5 μm particle size, 300 Å pore size) column was used on a Waters 600 HPLC system, and UV absorbance was monitored at 214 nm using a Waters 486 tunable absorbance detector. Samples were dissolved in 2 ml of buffer A (0.1 % TFA) and injected manually, and then the column was run at 100 % buffer A to wash off the concentrated salts present in the < 10 kDa fraction. The following gradient conditions of buffer B (90 % acetonitrile in 0.09 % TFA) were then used: 0–20 % in 5 min, 20–60 % over 40 min and then 60–80 % in 5 min. Molecular masses and purity of preparative RP (reverse-phase)-HPLC fractions were determined by MS analysis. ESI-MS data were acquired by manually injecting samples (10 μl of collected fractions) into the ESI-MS system and analysed in positive-ion mode.

Reduction and alkylation

Freeze-dried purified protein was dissolved (1 mg/ml) in denaturant buffer [6 M GdmCl (guanidinium chloride), 0.25 M Tris/HCl and 1 mM EDTA, pH 8.5]. To the mixture, 20 μl of 2-mercaptoethanol (Sigma) was added, followed by vortex-mixing and incubating under nitrogen at 37 °C for 2 h. After incubation, 100 μl of 4-vinylpyridine was added to the solution, followed by incubation at room temperature ($26 \pm 1\,^{\circ}C$) for 2 h. It was then subjected to RP-HPLC, and the protein was eluted. The reduction and alkylation of the protein were confirmed by checking the mass using ESI-MS. The native and reduced/alkylated proteins were sequenced using Edman degradation method on an Applied Biosystems 477A Protein Sequencer. The sequence was deposited in Swiss-Prot (http://www.expasy.org/cgi-bin/sprot-search-ful) under accession number P83952.

Design, construction and cloning of the synthetic gene

The protein sequence was back-translated to get the DNA sequence, and codons were optimized for overexpression in *E. coli*. This construct was designed to contain a 5′ BamHI site and a 3′ EcoRI site to clone in-frame into pET32a (Novagen). A start codon (ATG) was inserted at the 5′-end of the synthetic gene immediately before the protein sequence to facilitate CNBr cleavage after expression. To create the desired synthetic gene, two overlapping primers of 117 and 97 bases were synthesized (Proligo). Oligonucleotide A, a 117-mer (5′-GGATCCATGCATCATCATCATCATCATATGAAGGATCGTCCTAAGAAACCGGGACTTTGTCCTCCGCGGCCTCAGAAGCCGTGTGTTAAGGAATGCAAGAACGATGATAGCTGTCCC-3′) contained a hexahistidine tag and a start codon at the 5′ region and a 28-base overlap with oligonucleotide B at the 3′ region. Oligonucleotide B was a 97-mer (5′-GAATTCCTAGCCAACAAAAATAGGATCGCGACATTCATCCTTACAGCCATAGTTACAACACTTTTGTTGGGGACAGCTATCATCGTTCTTGCATTCC-3′) with a stop

codon at its 5′-end and a 28 bp overlap region at its 3′-end. Both oligonucleotides A and B contain six extra bases at their 5′-ends for restriction endonucleases BamHI and EcoRI respectively. Synthetic gene construction was based on a single-step method using PCR. The PCR mixture consisted of 0.4 unit of Advantage 2 Taq polymerase (Clontech), 0.4 μl of 10 mM of each oligomer, 0.4 μl of 10 mM dNTPs, 2 μl of 10 × PCR buffer in a total volume of 20 μl. The PCR conditions were as follows: one cycle of 94 °C for 2 min, 35 cycles of 94 °C for 30 s, 52 °C for 30 s and 72 °C for 20 s, and a final extension at 72 °C for 10 min. The PCR product was cloned into pGEMT-easy vector (Promega) and sequenced.

Fusion protein expression

The synthetic gene was double-digested with SacI and EcoRI (New England Biolabs) and cloned in-frame into pET32a which had been digested previously with the same restriction enzymes. This was sequenced again to confirm the fidelity and introduced into *E. coli* BL21/RIL strain. For expression, an overnight 50 ml culture of *E. coli* BL21/RIL harbouring pET32a/omwaprin was used to inoculate 1 litre of LB medium containing 1 mg/ml ampicillin and incubated at 37 °C with shaking until the cells reached the mid-exponential phase ($D_{600} = 0.4$–0.6). Fusion protein expression was then induced with 1 mM IPTG (isopropyl β-D-thiogalactoside) and incubated further at 37 °C with shaking for 6 h before the bacteria were harvested. Recombinant protein was analysed by SDS/PAGE on a 12 % (w/v) polyacrylamide gel. The expressed protein in the soluble fraction was purified from the bacterial lysate in a non-denaturing condition using BD TALON™ metal-affinity resin (Clontech) and then dialysed against MilliQ water.

Cleavage, purification and characterization of recombinant omwaprin

The freeze-dried protein was resuspended in 0.1 M HCl in the presence of 100-fold molar excess of CNBr (Sigma) over methionine residues and incubated at room temperature for 24 h. The solution was diluted 10-fold and freeze-dried to stop the reaction. Recombinant protein was purified to homogeneity using RP-HPLC on a Jupiter C_{18} column (10 mm × 250 mm, 10 μm particle size, 300 Å pore size) (Phenomenex) with solvent A (0.1 % TFA) and solvent B (80 % acetonitrile in 0.1 % TFA). The purity and folding of the recombinant protein was assessed by (i) chromatography and co-elution with native protein on a RP-HPLC Sephasil C_{18} column (Amersham Biosciences), (ii) ESI-MS, (iii) N-terminal sequencing, and (iv) CD.

CD spectrometry

Far-UV spectra (260–190 nm) of native and recombinant omwaprin were measured using Jasco J810 spectropolarimeter in MilliQ water (pH 7.4) at room temperature using 0.1 cm pathlength stoppered cuvettes. A total of three scans were recorded, averaged for each spectrum and baseline subtracted. The percentages of α-helix, β-sheet and random coil were calculated from the CD spectra using the method described at http://www.embl-heidelberg.de/~andrade/k2d/ [19].

Enzymatic cleavage to determine disulfide bridges

Approx. 50 μg of omwaprin was dissolved in 20 μl of 50 mM Tris/HCl and 6 M GdmCl, pH 8, and denatured for 1 h at 50 °C. After 1 h, the sample was diluted 6-fold with appropriate buffer depending on the proteinase used. Three proteinases, namely trypsin (Promega), pepsin and thermolysin (Sigma) were added at a 1:20 ratio of proteinase to omwaprin [20]. After overnight incubation at 37 °C (80 °C for thermolysin), the reaction mixture was subjected to RP-HPLC (as described above for the purification of recombinant omwaprin). The fractions were collected and freeze-dried, and were fully reduced by incubation in 50 μl of 50 mM Tris/HCl, 60 mM DTT (dithiothreitol) and 6 M GdmCl, pH 8, for 2 h at 37 °C. The reduced samples were diluted to 100 μl with 50 % acetonitrile and 0.1 % TFA for analysis by MALDI–TOF (matrix-assisted laser-desorption ionization–time-of-flight)-MS.

MALDI/TOF-MS

The samples containing the peptide fragments (0.5 μl) were spotted on to two 96-well plates and crystallized with 0.5 μl of matrix solution [5 mg/ml (w/v) CHCA (α-cyano-4-hydroxycinnamic acid), in 50 % acetonitrile and 0.1 % TFA] (Sigma). The samples were analysed on an AB 4700 Proteomics Analyzer MALDI–TOF/TOF mass spectrometer (Applied Biosystems). Peptide mass fingerprinting data were acquired automatically in the reflectron mode.

Partial reduction and cyanylation

To determine the disulfide linkages, partial reduction was carried out as described in [20] with modifications. Briefly, 0.5 mg of omwaprin in 0.5 ml of 0.05 % TFA and 30 % acetonitrile were incubated with 0.5 mol of TCEP [tris-(2-carboxyethyl)-phosphine]/cysteine in 0.5 ml of 0.1 M citrate buffer, pH 3.0, at 65 °C for 5 min. The protein solution and the reducing buffer were incubated at the same temperature before mixing. After cooling down to 25 °C, 20 mol of CDAP (1-cyano-4-dimethylaminopyridinium)/cysteine in 0.1 ml of 0.1 M citrate buffer, pH 3.0, was added to the mixture and cyanylation was accomplished by incubation for 15 min at 25 °C (TCEP and CDAP were bought from Sigma). The modified protein was purified by RP-HPLC using a Sephasil C_{18} column with a flow rate of 40 μl/min, monitoring absorbance at 215 nm, using a three-step gradient (0–20 % for 10 min, 20–45 % for 60 min and 45–100 % for 10 min) of solvent B. The HPLC fractions were collected manually and the components were analysed by MALDI–TOF/TOF-MS. The fractions corresponding to the reduced and cyanylated omwaprin were dried in a SpeedVac and kept at − 20 °C.

Cleavage of the cyanylated fractions

The cyanylated fractions were reconstituted to an approximate concentration of 1 mM in 30 % acetonitrile. A portion of the solution (5 μl) was mixed with an equal volume of 1 M NH_4OH (pH 12) and incubated at 25 °C for 1 h; excess NH_4OH was removed using a SpeedVac. After cleavage, the fragments were reduced completely using 0.1 M TCEP in 0.1 M citrate buffer, pH 3, for 30 min at 37 °C. The samples were diluted to 100 μl with 50 % acetonitrile and 0.1 % TFA for analysis by MALDI–TOF/TOF-MS [20].

Anti-proteinase activity

The proteinase-inhibitory effect of omwaprin was examined by studying its effect on the activity of elastase and cathepsin G. Elastase (50 nM in 100 mM Tris/HCl, pH 8) (Sigma) activity was measured by determining its amidolytic activity on the substrate Suc-Ala-Ala-Pro-Abu-*p*NA (0.4 mM) (Suc is succinyl, Abu is aminobutyric acid, and *p*NA is *p*-nitroanilide). Cathepsin G (30 nM in 50 mM sodium acetate and 150 mM NaCl, pH 5.5)

activity was measured using the substrate MeOSuc-Ala-Ala-Pro-Met-*p*NA (15 mM in DMSO) (MeOSuc is *N*-methoxysuccinyl). Proteinases were incubated with different concentrations of omwaprin (10 μM–1 mM) at 37 °C for 30 min. The residual proteinase activity was measured at 405 nm by the addition of the colorimetric substrate and incubation at 37 °C for 1 h [18].

Antibacterial assays

The antibacterial activity of omwaprin was evaluated using a sensitive two-stage radial diffusion assay [21]. Briefly, mid-exponential-phase bacteria from overnight cultures ($D_{620} = 0.4$), were centrifuged at 900 ***g*** for 10 min, washed and resuspended in 10 mM sodium phosphate buffer (pH 7.4) at 4 °C. The resuspended bacteria [$\sim 2 \times 10^6$ cfu (colony-forming units)/ml] added to autoclaved warm (40–50 °C) half-strength LB medium with 10 mg/ml low-melting-point agarose prepared in 10 mM sodium phosphate buffer, pH 7.4, served as the underlay gel. When high-ionic-strength underlay gel was needed, an additional 250 mM NaCl was added (350 mM final concentration). After mixing, the underlay gel was poured into sterile 90 mm × 15 mm Petri dishes to form a uniform layer of 2 mm depth. Evenly spaced wells were made using a 3 mm diameter biopsy punch, and 5 μl of control samples or different concentrations of protein in 10 mM sodium phosphate buffer were added to each well. Ampicillin (0.1 mg/ml) and 10 mM sodium phosphate buffer, pH 7.4, were used as the positive and negative controls respectively. The plates were incubated for 2 h at optimum temperature for each bacterial strain and overlaid with 10 ml of full-strength LB medium and 10 mg/ml low-melting-point agarose. After incubation for 12–18 h at 37 °C, the diameter of the clear zone surrounding each well was measured under an Olympus SZ40 Zoom Stereo Microscope. The rapidly growing *Bacillus megaterium* required only approx. 6 h of incubation for the assay, whereas all other strains were kept for overnight incubation. The antibacterial activity was calculated as the difference between the diameter of the clear zone containing the protein sample and that of the negative control (3 mm).

SEM (scanning electron microscopy)

The structural changes produced by omwaprin on *Bacillus megaterium* and *Staphylococcus warneri* were studied by SEM using the method of Yenugu et al. [22] with slight modifications. Briefly, bacteria (10^7 cfu/ml) were resuspended in 10 mM sodium phosphate buffer, pH 7.4, treated with 500 μM and 1 mM omwaprin and incubated for 1–3 h at 37 °C. After incubation, the bacteria were washed and fixed overnight at 4 °C with 2.5 % (v/v) glutaraldehyde (Sigma). Following fixation, the cells were mounted on coverslips using poly(L-lysine) and rinsed with 10 mM sodium phosphate buffer, pH 7.4, and dehydrated through an ethanol series. The samples were dried at 37 °C and coated with 10–15 nm thickness of gold/palladium (60:40) alloy using a BAL-TEC SCD-005 sputter coater. Samples were examined using a JEOL 5600 LV scanning electron microscope with an accelerating voltage of 10 kV.

Haemolytic activity assay

The haemolytic activity of the protein was tested using human erythrocytes [23]. A 2.5 % (v/v) suspension of washed erythrocytes in PBS was incubated with omwaprin ranging from 10 μM to 1 mM in a 96-well plate for 2 h with intermittent shaking. The absorbance in the supernatant was measured at 415 nm. Haemolysis caused by PBS and 1 % (v/v) Triton X-100 were used as 0 and 100 % controls respectively.

Homology modelling

Since omwaprin shows 38 % sequence identity with nawaprin, with all of the cysteine residues and several proline residues conserved when aligned using DNAMAN (Lynnon BioSoft), the nawaprin structure was used as a template for homology modelling. SWISS-MODEL, an automated protein modelling server (http://www.expasy.ch/swissmod/SWISS-MODEL.html), was used to obtain a preliminary three-dimensional structural model of omwaprin. However, residues 1–5 and 44–50 and two disulfide bonds (Cys^5–Cys^{30} and Cys^{23}–Cys^{38}) were missing in the model because of the absence of conserved residues at the C- and N-termini for aligning. Insight II software (Accelrys) was used to build the remaining part and model the molecule on a Silicon Graphics workstation [24]. The missing residues and two disulfide bonds were incorporated using the biopolymer module. The model was subjected to energy minimization using the steepest descent method (100 steps) followed by the conjugate gradient method until the rmsd (root mean square deviation) was 0.5 kcal/mol Å (1 kcal ≈ 4.184 kJ). The resulting structure was checked for bond length and bond angle consistency as well as 'ω' peptide bond. All the peptide bonds were *trans*, including the Xaa–Pro peptide bond. The quality of the final structure was evaluated using Ramachandran map (Φ, ψ-plot).

Mutagenesis

Six N-terminal residues of omwaprin were deleted by PCR mutagenesis. The omwaprin gene was amplified using the primers mutOF, 5′-GACGACGACAAGATGCCGGGACTTTGTC-3′, and mutOB, 5′-GAGGAGAAGCCCGGTTACTAGCCAAC-3′, and cloned into pET32 Ek/LIC vector (Novagen). Expression, purification and characterization of the mutant protein were carried out using a similar strategy as described above for the complete protein. The mutant protein was characterized by ESI-MS and CD.

RESULTS

Identification of a novel protein from inland taipan venom

LC–MS analysis of *Oxyuranus microlepidotus* centrifuge-filtered venom revealed a component with a molecular mass of 5602 Da (see Supplementary Figures S1A and S1B at http://www.BiochemJ.org/bj/402/bj4020093add.htm). This protein was purified by RP-HPLC of the filtrates containing < 10 kDa components of the venom. The purified protein was reduced and alkylated before sequencing. The sequence of the protein and its reduction and alkylation were verified by comparing the calculated and observed masses (Supplementary Figure S1C). The observed molecular masses matched the calculated masses. As it shows similarity to waprins [12], we named it as omwaprin (*Oxyuranus microlepidotus* waprin). The protein sequence was deposited in Swiss-Prot under accession number P83952. Omwaprin shows 37–41 % sequence similarity to nawaprin, a snake venom waprin [12], and other WAP domain proteins [12] such as elafin, SLPI, WAP and SWAM1 (Figure 1).

Design, construction and expression of synthetic gene

In order to study the biological functions, structure and structure–function relationships, milligram quantities of omwaprin are required. Since omwaprin occurs in low quantities in the snake venom, we resorted to recombinant protein production for our analyses. A synthetic gene (189 bp) encoding omwaprin with preferred codons for *E. coli* expression was designed (Figure 2A).

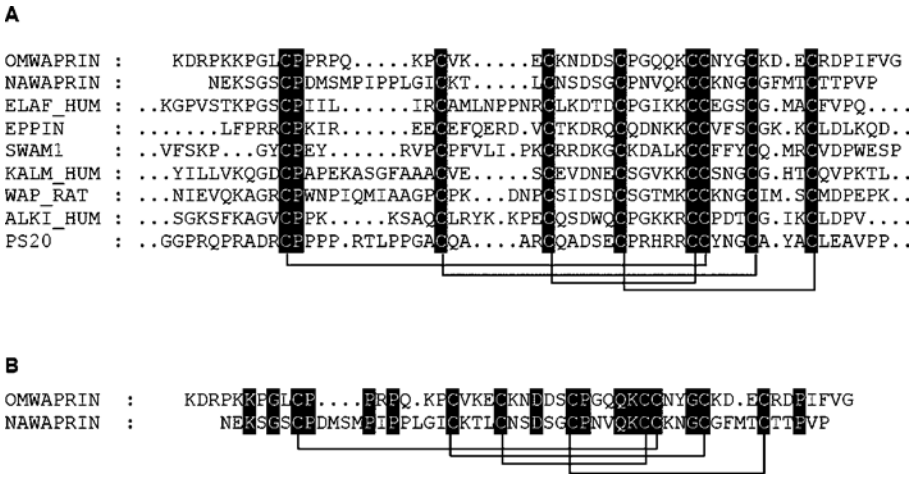

Figure 1 Amino acid sequence of omwaprin

(**A**) Sequence similarity of omwaprin with other WAP family members. Identical residues are marked in black. The lines connecting corresponding cysteine pairs show the disulfide-bonding pattern. (**B**) Structural similarity of omwaprin to that of nawaprin. Identical residues are shown in black boxes. Lines as in (**A**).

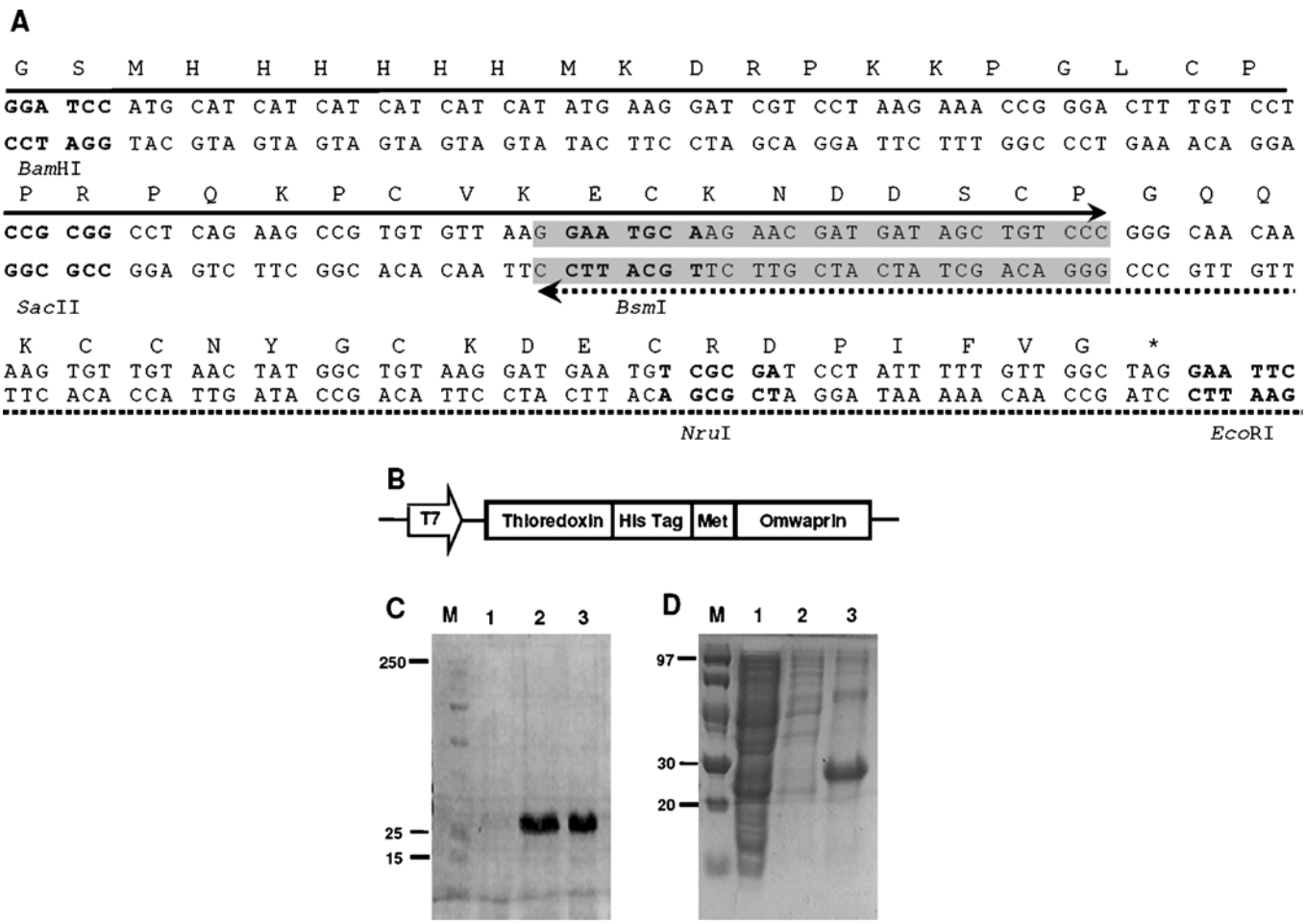

Figure 2 Design, construction, cloning and expression of a synthetic gene for omwaprin

(**A**) Full-length sequence of synthetic gene. Three unique restriction enzyme sites are shown in bold letters, and the amino acid sequence is shown above the DNA sequence. Solid and broken arrows represent two oligonucleotides with an overlapping region of 28 bp (shown in shaded box). (**B**) Schematic representation of the construct showing thioredoxin–omwaprin fusion. Met indicates CNBr cleavage site. (**C**) SDS/PAGE analysis of expression of fusion protein in *E. coli* BL21(RIL). Lane M, molecular-mass marker (sizes in kDa); lane 1, before IPTG induction; lanes 2 and 3, 1 and 6 h after induction. (**D**) Purification of fusion protein on BD-TALON™ metal-affinity resin. Lane M, molecular-mass marker (sizes in kDa); lane 1, column flow-through; lane 2, buffer wash; lane 3, 150 mM imidazole wash.

Unique internal restriction sites that may be helpful for future structure–function studies were included in the designed gene. The synthetic gene was constructed by an overlapping fill-in method using PCR (Figure 2A). After confirming the sequence, recombinant omwaprin was expressed in *E. coli* BL21-RIL using the pET32a vector (Figure 2B). The protein was present in the soluble fraction when induced with 1 mM IPTG as indicated by a thick band of ~25 kDa on SDS/PAGE analysis (Figure 2C). Optimization of the expression was accomplished by varying different parameters such as bacterial strains, temperature and incubation time (results not shown).

Purification and cleavage of recombinant protein

The soluble recombinant protein was purified from the bacterial cell lysate using BD TALON™ metal-affinity resin. The His_6-tag attached to the protein aided a one-step purification using cobalt-affinity chromatography (Figure 2D). The purified protein was then dialysed against MilliQ water and freeze-dried. After cleaving the fusion protein using CNBr, recombinant omwaprin was purified to homogeneity using RP-HPLC (see Supplementary Figures S2A and S2B at http://www.BiochemJ.org/bj/402/bj4020093add.htm). The identity of the protein was confirmed by ESI-MS and N-terminal sequencing. Recombinant omwaprin showed a mass of 5602.0 ± 0.7 Da, which matched well with that of the native protein. Also, eight N-terminal residues of recombinant omwaprin (KDRPKKPG), verified by N-terminal sequencing, matched with that of native omwaprin.

Characterization of recombinant omwaprin

The folding of recombinant omwaprin was evaluated by co-elution and CD. Co-elution was performed using RP-HPLC on a Sephasil C_{18} column. Recombinant and native proteins were eluted at the same concentration of acetonitrile (buffer B) and showed the same retention time (Supplementary Figure S2C). Furthermore, they were co-eluted when a mixture of equal amounts of recombinant and native omwaprin were injected. The CD spectra of both native and recombinant omwaprin showed a similar negative ellipticity value near 200 nm, suggesting that both have a similar folding (Supplementary Figure S2D). The percentages of random coil, α-helix and β-sheet in the secondary structures were 48, 5 and 47 respectively.

Disulfide linkages in omwaprin

Experiments were carried out to determine the disulfide bonds in omwaprin. Our initial efforts by proteolytic cleavage and MS analysis failed, as omwaprin was resistant to the proteinases tested (Supplementary Table S1 at http://www.BiochemJ.org/bj/402/bj4020093add.htm). Hence, an alternative strategy of partial reduction and cyanylation was employed to determine the cysteine connectivity. Partial reduction of omwaprin was carried out using TCEP and was optimized with respect to the incubation temperature and time to give the highest ratio of partially reduced disulfide species relative to fully reduced protein. The cyanylation of thiol groups was carried out using CDAP at acidic conditions to minimize thiol/disulfide exchange. The reduced and cyanylated proteins were eluted after the unmodified native protein on RP-HPLC (Supplementary Figure S3A at http://www.BiochemJ.org/bj/402/bj4020093add.htm). Two peaks corresponding to singly reduced and cyanylated isomer were identified by MALDI–TOF/TOF analysis (indicated as peaks 1 and 2 in Supplementary Figure S3A). These singly reduced and cyanylated isomers showed a mass of $M\mathrm{H}^+ = 5652.3$ Da (Supplementary Figure S3B).

Table 1 Disulfide assignment by peptide mapping of cleavage mixtures of reduced and cyanylated isomers

Calculated *m/z* values of possible fragments resulting from CN-induced cleavage of singly reduced and cyanylated species of omwaprin isomers compared with experimental data.

	Average [$M\mathrm{H}^+$]			
HPLC peak	Calculated	Observed	Peptide fragment	Disulfide assignment
1	1941.11	1941.12	1–17	Cys^{18}–Cys^{39}
	2346.90	2347.63	Itz-(18–38)	
	1406.62	1405.71	Itz-(39–50)	
2	1700.63	1700.13	Itz-(28–42)	Cys^{28}–Cys^{43}
	931.44	931.43	Itz-(43–50)	
3a	1037.63	1037.65	1–9	Cys^{10}–Cys^{35}
	1843.75	1843.74	Itz-(35–50)	
3b*	1347.54	1372.68	Itz-(22–33)	Cys^{22}–Cys^{34}
	1946.76	1946.08	Itz-(34–50)	

*Peptide mapping of cleavage mixture of doubly reduced and cyanylated isomer.

An additional peak containing a mixture of singly and doubly reduced and cyanylated omwaprin ($M\mathrm{H}^+ = 5652.3$, 5702.55 Da) was also detected (peak 3 in Supplementary Figure S3A). It was rechromatographed by RP-HPLC to separate the singly and doubly reduced and cyanylated isomers (labelled 3a and 3b respectively in Supplementary Figure S4 at http://www.BiochemJ.org/bj/402/bj4020093add.htm).

After freeze-drying, the cyanylated samples were cleaved using 1 M NH_4OH, and samples were fully reduced to break all residual disulfide bonds by incubation with TCEP and analysed by MALDI–TOF/TOF (see Supplementary Figure S5 at http://www.BiochemJ.org/bj/402/bj4020093add.htm). The calculated *m/z* value for $M\mathrm{H}^+$ of each of the possible CN-induced cleavages (cleavage by aqueous ammonia at the N-terminus of cyanylated cysteine residues) fragments resulting from all possible singly cyanylated species were compared with the *m/z* signals from singly reduced and cyanylated isomers. On the basis of the unique masses of the fragments from the singly reduced and cyanylated isomers, peaks 1 and 2 in Supplementary Figure S3A and peak 3a in Supplementary Figure S4 can be assigned to the products of CN-induced cleavage at Cys^{18}–Cys^{39}, Cys^{28}–Cys^{43} and Cys^{10}–Cys^{35} respectively (Table 1). The fourth disulfide bond was confirmed by analysing the peak 3b (Supplementary Figure S4, peak corresponding to doubly reduced and cyanylated isomer obtained by re-chromatography of peak 3). The observed unique mass 1372.62 Da can be attributed to the fragment itz-(22–33) (itz is iminothiazolidine). However, this mass was 25.08 Da higher compared with the calculated mass of 1347.54 Da. This increased mass could be due to an additional cyanylation at Cys^{28} and incomplete CN-induced cleavage. Similar kinds of incomplete CN-induced cleavage were reported previously [25]. The use of TCEP and CDAP as reducing and cyanylating agents respectively is beneficial, as they are compatible with acidic pH, hence minimizing disulfide scrambling [20]. Furthermore, because of the optimized cleavage conditions used, we did not detect undesirable fragments with masses deviating by more than 2.5 kDa resulting from potential β-elimination reactions.

Our initial experiments to reduce omwaprin using denaturing buffers, such as 0.1 M citrate buffer or 6 M GdmCl, yielded either intact protein or completely reduced omwaprin at different incubation times and temperatures tested. A careful optimization of reduction conditions was needed, because the molecule might become more accessible for complete reduction after the breakage of the initial few disulfide bridges. Several reduction conditions were carefully explored to obtain significant amounts of singly

reduced isoforms. The disulfide bridges are similar to those of nawaprin and other WAP domains [12].

In vivo toxicity

To examine the general toxicity of omwaprin, it was injected intraperitoneally into Swiss albino male mice (20 ± 2 g) with doses of up to 10 mg/kg. No abnormal behaviour or symptoms were observed in the mice injected with omwaprin, and they remained comparable with the control mice during a 24 h observation period.

Proteinase-inhibitory effect

Many of the WAP domain proteins, such as elafin [16] and SLPI [17], show a proteinase-inhibitory effect. In order to investigate whether omwaprin is a proteinase inhibitor, the residual activity of elastase and cathepsin G was tested after incubating with the protein. No inhibition of proteinase activity was observed for omwaprin even at 1 mM, whereas, according to earlier reports, the IC_{50} values of elafin and SLPI are in the nanomolar range [19].

Antimicrobial activity

Since many WAP domain proteins are reported to have antibacterial property, omwaprin was tested for antibacterial activity by radial diffusion assay. *B. megaterium*, *B. thuringiensis*, *Strep. clavuligerus*, *Staph. aureus*, *Staph. warneri*, *E. coli* and *A. tumefaciens* were used as target bacteria. Omwaprin showed a concentration-dependent antibacterial activity against selected Gram-positive strains such as *B. megaterium* and *Staph. warneri*. The control, 10 mM sodium phosphate buffer without protein, gave no clear zone. The MID (minimum inhibitory dose) was calculated, which was the minimum dose of omwaprin forming a detectable zone of clearance larger than the size of the negative control (3 mm) under experimental conditions [21]. The MID was 2.8 μg (560.2 μg/ml) for *B. megaterium* and 8.5 μg (1.7 mg/ml) for *Staph. warneri* (Figure 3A). However, omwaprin did not show any antibacterial effect on the other three Gram-positive strains tested, *B. thuringiensis*, *Staph. aureus* and *Strep. clavuligerus*, or on the Gram-negative strains even at a dose of 28 μg (5.6 mg/ml). Omwaprin showed approx. 10–15-fold lower antibacterial activity than ampicillin on *B. megaterium* when equimolar concentrations were compared (results not shown).

Since the antibacterial activities of several proteins are affected by high salt concentrations [26], radial diffusion assays were performed to evaluate the effect of NaCl on the activity of omwaprin. The antibacterial property was comparable in the presence and absence of extra 250 mM NaCl (Figure 3B). Thus omwaprin possesses salt-tolerant antibacterial activity.

Morphological changes induced by omwaprin

In order to study the mechanism of action of omwaprin, morphological changes induced by the protein on bacteria were studied by SEM. Representative micrographs of selected experiments are shown in Figure 4. Control bacterial cells had a smooth and normal surface morphology (Figures 4A–4C). Incubation of *B. megaterium* with 14 μg (2.8 mg/ml) (Figures 4D–4F) and 28 μg (5.6 mg/ml) (Figures 4G–4I) omwaprin showed severe membrane damage, including membrane wrinkling, blebbing and subsequent leakage of cytoplasmic contents. The majority of the cells lost their shape and membrane integrity after the treatment. Similar structural changes in morphology were observed for *Staph. warneri* (Figures 4J–4L), whereas no morphological changes were observed in the case of *E. coli* and *Staph. aureus*, representatives of non-susceptible Gram-negative and Gram-positive bacteria respectively (results not shown).

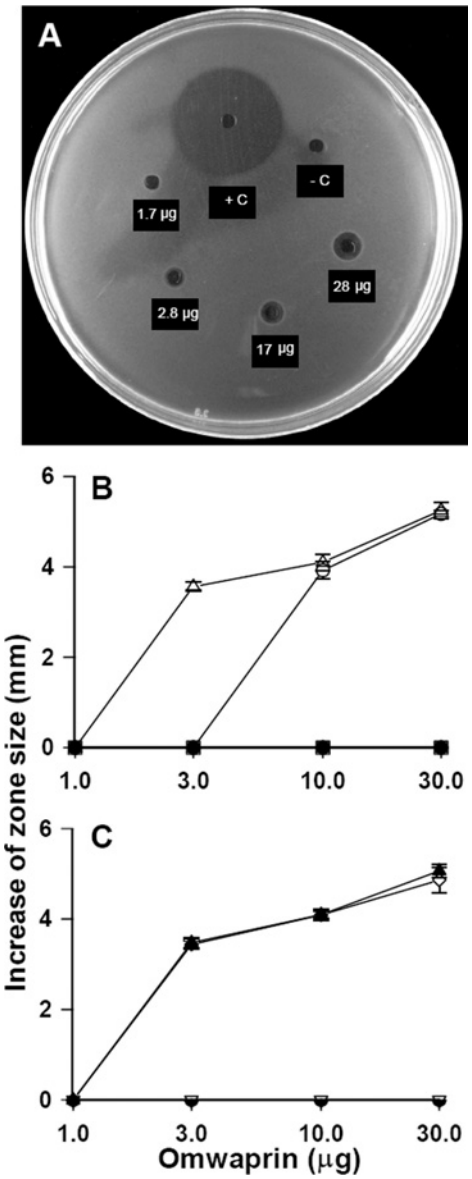

Figure 3 Antibacterial activity of recombinant omwaprin

(**A**) Radial diffusion assay. *B. megaterium* at 2×10^5 cfu was incorporated into LB agarose medium. Samples (5 μl in 10 mM sodium phosphate buffer, pH 7.4) containing doses ranging from 0.85 to 28 μg (30 μM to 1 mM) were added into each well (3 mm diameter), and the plates were incubated for 2 h to allow the samples to diffuse into the agarose, before pouring a nutrient-rich overlay gel. Antibacterial activity of omwaprin, represented by clear zones surrounding the wells, is dose-dependent. The negative control (buffer only, $-$C) gave no clear zone, while the positive control (0.1 g/l ampicillin, $+$C) showed a prominent clear zone around the well. (**B**) Antibacterial activity of omwaprin against *B. megaterium* (△), *Staph. warneri* (○), *B. thuringiensis* (★), *Staph. aureus* (□) and *Strep. clavuligerus* (●) in a radial diffusion assay. The diameters of the clear zones were measured and plotted after subtracting the diameter of the well (3 mm). Results are means $\pm$ S.D. for three independent assays each performed in triplicate. (**C**) Salt-sensitivity and structural dependence of omwaprin antibacterial activity. Activity against *B. megaterium* under high-salt (350 mM) (▲) and low-salt (100 mM) (◇) conditions. The antibacterial activity appears to be independent of salt concentration. Effect of reduced and alkylated omwaprin (▽) against *B. megaterium*: unfolded omwaprin lost the antibacterial effect, indicating that disulfide bonding and proper folding are important for its antibacterial activity. Effect of mutant omwaprin (▾) against *B. megaterium*: mutant protein failed to show antibacterial activity, showing that N-terminal cationic residues are essential for its activity.

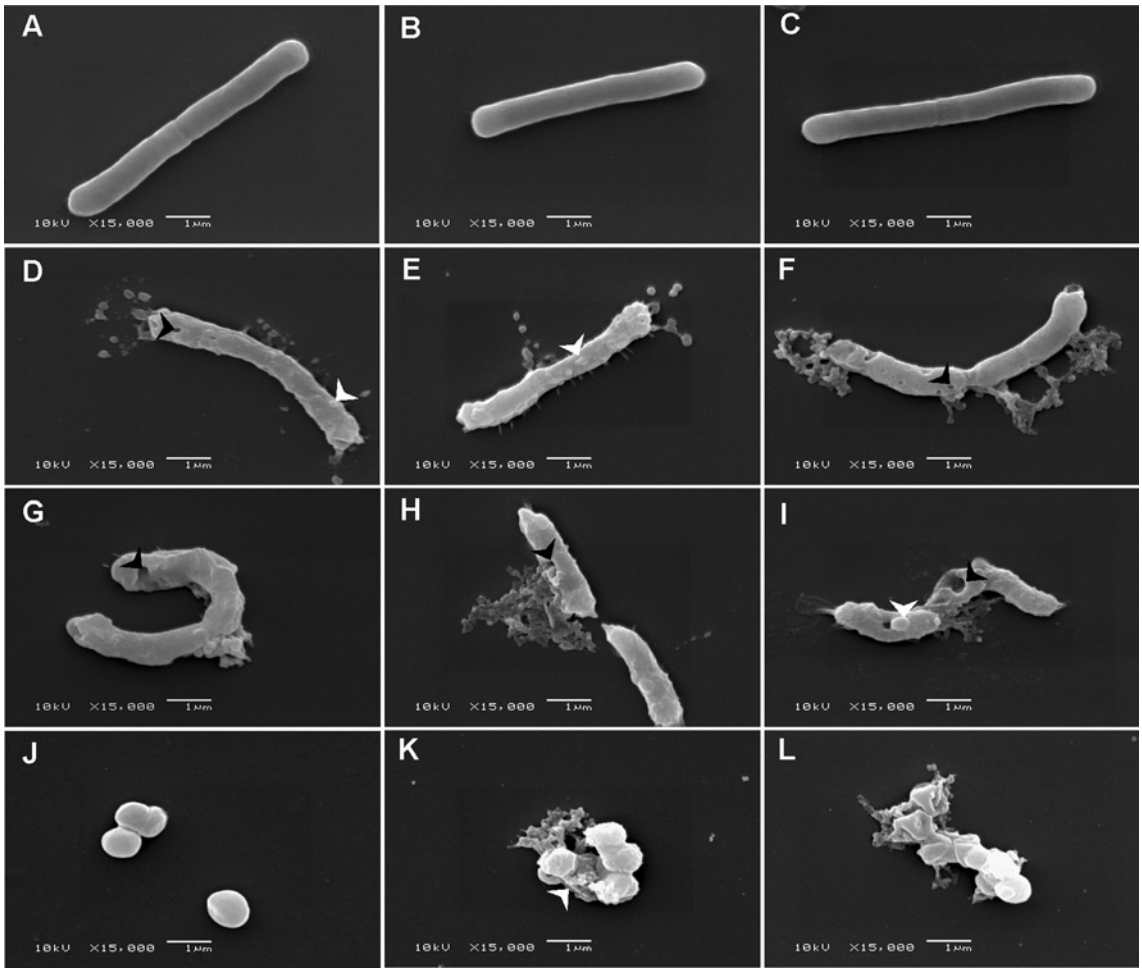

Figure 4 Scanning electron micrographs of omwaprin-treated *B. megaterium* and *Staph. warneri*

B. megaterium incubated at 31 °C for 1 h (**A**, **D** and **G**), 2 h (**B**, **E** and **H**) or 3 h (**C**, **F** and **I**), without omwaprin (**A**–**C**), with 500 μM (2.8 mg/ml) omwaprin (**D**–**F**), with 1 mM (5.6 mg/ml) omwaprin (**G**–**I**). The images show membrane blebbing and pore formation with leakage of cellular contents highlighted with white and black arrowheads respectively. *Staph. warneri*, incubated for 1 h with 0 μM (**J**), with 500 μM (**K**) and with 1 mM (**L**) omwaprin.

Haemolytic activity

To investigate whether omwaprin has any effect on mammalian membranes, its haemolytic effect was tested. After incubating human erythrocytes with the protein up to 1 mM concentrations, no haemoglobin release was observed, indicating that omwaprin does not cause lysis of erythrocyte membrane (results not shown).

Structure–function relationship studies

Disulfide bridges and overall conformation are required for biological activities of many cysteine-rich proteins, such as the antibacterial properties of β-defensins [27]. To determine the importance of disulfide bonds and folding for the antibacterial properties of omwaprin, the disulfide bonds were reduced and alkylated. The denatured omwaprin failed to show any antibacterial activity even at a dose of 28 μg (5.6 mg/ml) on *B. megaterium*, as demonstrated by radial diffusion assay (Figure 3B). The results indicate that disulfide-bond-constrained tertiary structure is essential for the antibacterial function of the protein.

A three-dimensional model of omwaprin was built using the known structure of nawaprin [12], since it shows 38 % identity, with all of the cysteine residues and several proline residues conserved (Figure 1B). The partial reduction and cyanylation experiments proved that both omwaprin and nawaprin show similar disulfide pairing. Furthermore, CD studies show that both the proteins possess a similar secondary structure (results not shown). The energy-minimized homology model of omwaprin is shown in Figures 5(A)–5(C). The final minimized structure had ϕ and ψ values within the allowed region of the Ramachandran map. A total of 22 residues (46.80 %) were in the fully allowed region, 18 residues (38.30 %) were in the additionally allowed region, five residues (10.64 %) were in the generously allowed region and only two glycine residues (4.26 %) were in the outside region (results not shown).

The omwaprin model shows similarity to the structure of nawaprin, consisting of spiral backbone conformation with two circular segments connected by four disulfide bonds [12]. The structure consists of two β-turns which are situated at residues 24–27 and 37–40. The outer segment incorporates an antiparallel β-sheet at residues 35–37 and 41–43. The remaining part of the molecule is loop-structured. Both the N-terminal and C-terminal parts of the protein project out of the flat disc-like circular segments (Figure 5C). The analysis of the electrostatic potential of the molecule reveals that the charge distribution is distinct. The omwaprin structure model shows that the N-terminal part

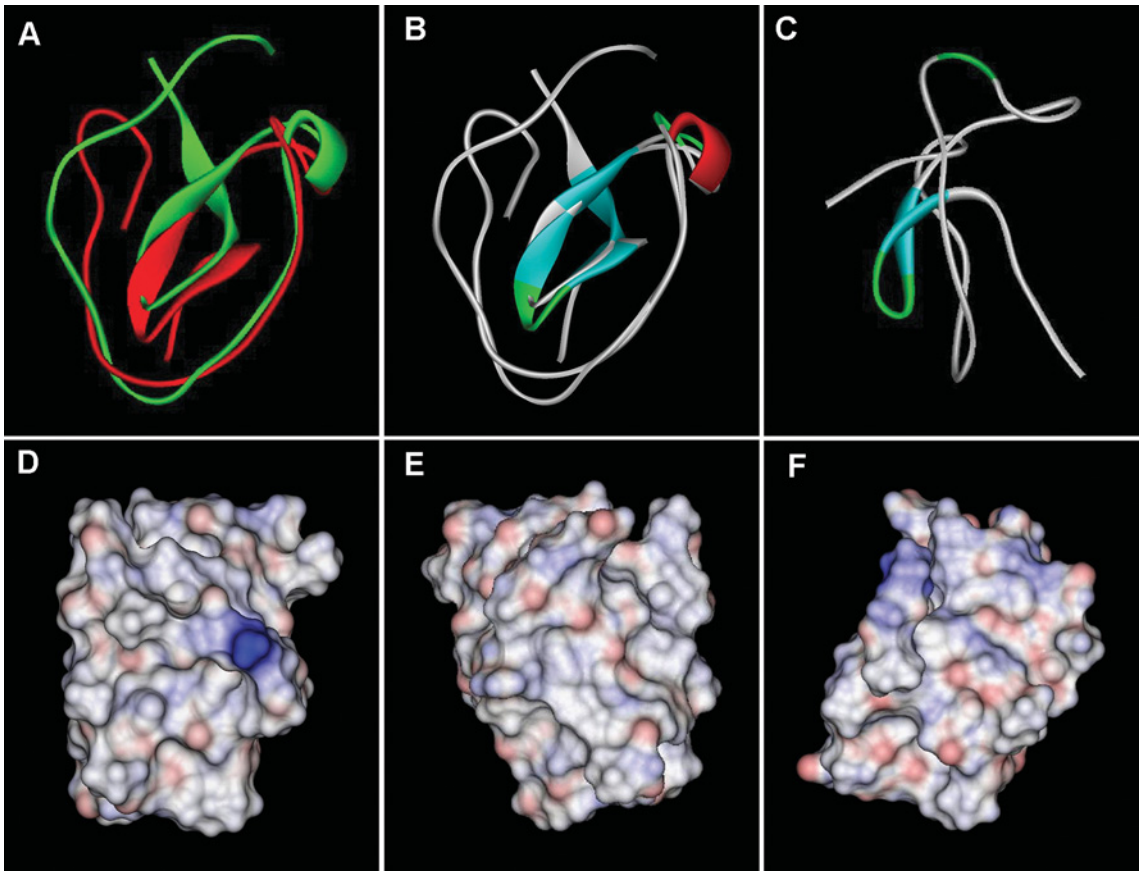

Figure 5 Homology modelling of omwaprin

Comparison of omwaprin and nawaprin structures. (**A**) Omwaprin (red) and nawaprin (green) structures were superimposed over the backbone atoms. (**B**) Ribbon structure of omwaprin and nawaprin (blue, green and red represents β-sheets, β-turns and α-helix respectively). (**C**) Ribbon structure of omwaprin in a different view related by $\sim$90° rotation about (**B**). (**D**, **E**) Molecular surface of omwaprin highlighted to show electrostatic potential, surfaces with positive, negative and neutral electrostatic potentials are drawn in blue, red and white respectively. Front and back views, $\sim$180° with respect to each other, are shown. The N-terminal segment shows maximum positive charge localization represented by the intense blue colour. (**F**) Front view of the mutant protein without the six N-terminal residues lacking the positive charge segment.

of the molecule harbours maximum surface positive charge (Figures 5D and 5E), which is essential for the antibacterial activity of the protein (see below).

The N-terminal region of omwaprin preceding the cysteine loops comprises four positively charged residues out of nine residues (KDRPKKPGL). In order to determine whether this charged 'tail' contributes to the antibacterial property, deletion mutagenesis was carried out. The mutant protein with a six-amino-acid deletion showed a mass of 4845.87 ± 0.01 Da by ESI-MS, which was comparable with the calculated mass of 4845.6 Da. The secondary structure of mutant omwaprin showed a fold similar to that of omwaprin, as supported by CD analysis (results not shown). The mutant that lacked the N-terminal cationic segment (Figure 5F) did not show antibacterial activity (Figure 3C) even at a dose of 28 μg (5.6 mg/ml), indicating that the positively charged N-terminal residues play a key role of in its activity.

DISCUSSION

We have described the isolation and functional characterization of omwaprin, a new member of waprin family, from the venom of inland taipan (*Oxyuranus microlepidotus*). Omwaprin contains a WAP domain within its mature protein size of 50 amino acid residues. The small size of the protein ($\sim$50 amino acid residues) and the presence of the characteristic arrangement of eight cysteine residues are distinguishing features of members of the waprin family [12]. CD spectral analysis (results not shown), determination of disulfide bridges and homology modelling of omwaprin showed that its overall fold is similar to that of nawaprin, the first member of this family. This is expected given a sequence similarity of 38 % and the presence of conserved cysteine residues. The inter-cysteine segments are divergent among waprins, as in other WAP domain proteins, hence they may have a variety of functions. The biological function of nawaprin is still unknown [12].

Owing to the small size and the typically high evolutionary rate of snake venom components, omwaprin and nawaprin are phylogenetically distinct from each other and are members of an unresolved peptide family [28]. However, sequence alignment of omwaprin and nawaprin showed that, in addition to the cysteine residues, many other residues such as proline, glycine and lysine are also conserved along the sequence (Figure 1B). Since the cysteine and proline residues are crucial factors for determining protein folding, the proteins may have similar structures.

The disulfide-bonding pattern of omwaprin was determined experimentally as Cys^{18}–Cys^{39}, Cys^{28}–Cys^{43}, Cys^{10}–Cys^{35} and Cys^{22}–Cys^{34}. Omwaprin contains very few suitable proteinase cleavage sites between the cysteine residues. Also, omwaprin shows high resistance to proteinases, which may be due to its

highly compact folding stabilized by disulfide bonds. Owing to these limitations, our attempts to determine the disulfide bridges of omwaprin using the traditional method of enzyme digestion and MS failed. So we decided to use the strategy of partial reduction and cyanylation. In this method, a water-soluble reducing agent, TCEP, was used under optimized conditions so that singly reduced isoforms were obtained which were cyanylated *in situ* by CDAP [29]. Three expected peaks corresponding to singly reduced and cyanylated isoforms were identified by RP-HPLC. However, a peak corresponding to the expected fourth singly reduced and alkylated omwaprin isomer was absent from our experiment, which may be because of lower stability of the isoform after reduction and cyanylation. Nevertheless, the fourth expected isomer was identified as a doubly reduced and cyanylated form. Hence the data from partial reduction and cyanylation experiments showed that omwaprin possesses similar disulfide bonds, as suggested by its sequence similarity to other WAP domain proteins, especially elafin and nawaprin [12,16].

The omwaprin model superimposed over the backbone residues of nawaprin using Swiss-Pdb viewer (http://www.expasy.org/spdbv) is shown in Figures 5(A) and 5(B). The tertiary folds of the proteins are similar, as indicated by the similarity in disulfide-bond pairing. Furthermore, the locations of β-sheets are in the internal segments for both proteins. Even though the proteins show sequence similarity to proteinase inhibitors such as elafin [16] and SLPI [17], they do not have any effect on the activities of proteinases such as elastase and cathepsin G (results not shown).

The main differences between omwaprin and nawaprin are: (i) the presence of $+4$ net charge in the case of omwaprin, but $+1$ in the case of nawaprin under physiological conditions; (ii) omwaprin has a comparatively longer N-terminal region beyond the cysteine loops consisting of four positively charged residues out of nine residues (KDRPKKPGL); our structure–function relationship studies demonstrated that this charged 'tail' contributes to its antibacterial property (see below); and (iii) seven of the 'best' 20 structures of nawaprin possess a 3_{10} helix spanning residues in the outer segment instead of a β-turn in omwaprin model [12] (Figure 5B).

The antibacterial property of other WAP domain proteins such as elafin [16], SWAM1 and SWAM2 [19], EPPIN (epididymal proteinase inhibitor) [30] and eNAP-2 (equine neutrophil antibiotic peptide 2) fragment [31] suggested that omwaprin may have antibacterial activity. Omwaprin shows dose-dependent antibacterial activity against selected Gram-positive bacteria. The activity of antibacterial proteins is normally affected by various factors such as their amino acid sequence, net charge of the protein, three-dimensional structure, bacterial membrane composition and salinity of the environment. High salt concentrations interfere with the electrostatic interactions between the cationic protein and bacterial membrane and inhibit the activity of some antibacterial proteins, including neutrophil defensins [32]. However, omwaprin maintained its antibacterial activity even in the presence of 350 mM NaCl. Compared with other cationic salt-sensitive proteins, the retention of activity at high salt concentrations suggests distinct electrostatic interactions between the protein molecule and the bacterial membrane. The residues that may be contributing to the salt-tolerant activity of omwaprin are still unknown. Similar salt-tolerant activity was reported for HE2 (human epididymis 2) proteins [27].

The mechanism of antibacterial action was by affecting the membrane integrity, as indicated by our SEM analyses of bacteria treated with approx. 5- and 10-fold MID of omwaprin for 1, 2 and 3 h. Similar effects were observed for antibacterial proteins such as HE2 protein isoforms [33] and human β-defensin [32]. The mode of action of cationic proteins that affect Gram-positive bacteria is thought to be due to their interaction with the cytoplasmic membrane, its ultimate disruption and leakage of cytoplasm, resulting in cell death. Depolarization of cytoplasmic membrane of *Micrococcus luteus* by synthetic tick defensin has been demonstrated using a $diSC_3$-5 (3,3′-dipropylthiadicarbocyanine iodide) assay [34]. Antibacterial mechanisms of neopteran insect defensins are also reported to be through disruption of cytoplasmic membrane [35]. The outer membrane of Gram-negative bacteria inhibits the antibacterial activity of brochocin-C and nicin by preventing access of the protein to the cytoplasmic membrane [36]. In the present study, two Gram-negative strains of bacteria were not susceptible to omwaprin, suggesting that omwaprin may be targeting bacterial cytoplasmic membrane for its activity. Generally, the mechanism of action of cationic antibacterial proteins on cytoplasmic membrane does not seem to involve specific receptors as indicated by the retention of antibacterial activity by the D-enantiomers of three naturally occurring, pore-forming, antibacterial peptides cecropin A, magainin 2 amide and melittin [35]. The exact mechanisms involved in membrane binding and ultimate death of bacteria are still unclear [37].

Omwaprin shows species-specific antibacterial activity on Gram-positive bacteria tested. It shows activity against two Gram-positive strains *B. megaterium* and *Staph. warneri*, whereas it does not show activity against three other Gram-positive and Gram-negative bacteria tested. This selective antibacterial activity may be due to several factors, including charge density and structure of lipopolysaccharides in the case of Gram-negative bacteria, or lipid composition of the cytoplasmic membrane and the electrostatic potential across this membrane in Gram-positive bacteria. Also, peptide transport and efflux mechanisms may lead to species-selectivity of such antibacterial proteins [37]. Further experiments are needed to identify the wider spectrum of resistant and susceptible strains of bacteria. The C-terminal tail sequence of omwaprin with multiple hydrophobic residues (RDPIFVG) shows similarity to C-terminal sequences of several antibacterial proteins from insects, including cathelicidins, pyrrhocoricin, drosocin and apidaecin. The hydrophobic tail of cathelicidin is suggested to have a role in the process of initial interaction with the target bacteria [38]. It remains to be seen whether such strain-specificity is defined by the C-terminal tail in omwaprin.

Some of the antibacterial WAP domain proteins also have anti-proteinase activity. For example, both elafin and SLPI show antibacterial as well as anti-proteinase activities. In contrast, omwaprin and other WAP domain antibacterial proteins such as SWAM1 and SWAM2 [18] lack proteinase-inhibitory activity. Similar to omwaprin, the WAP domain antibacterial proteins, including elafin [16], SWAM1 [19] and EPPIN [27], possess net positive charges ranging from $+5$ to $+7$, except SWAM2, which has a net negative charge. However, the pattern of charge distribution among these antibacterial proteins is different. The omwaprin structure model shows the localization of positive charges at a single area on the surface of the molecule (N-terminal), which is essential for its antibacterial activity (Figure 5D). However, positive charges are distributed in the case of elafin [12]. Although omwaprin shows 33–41 % identity with other WAP domain antibacterial proteins, there are hardly any conserved residues other than cysteines and one proline residue, unlike the case of mammalian α-defensin family where a pair of oppositely charged residues Arg^5 and Glu^{13} and are conserved which are essential for their activity [26].

Many antibacterial proteins such as melittin [39], LL-37 [40] and SMAP-29 (sheep myeloid antimicrobial peptide 29) [41] can affect eukaryotic membranes as well. The lack of haemolytic activity on human erythrocytes observed in the present study

demonstrates the selectivity of omwaprin to bacterial compared with eukaryotic membranes. Glukhov et al. [42] recently demonstrated that water-soluble cationic proteins containing positively charged tags cannot leave the bulk water for attachment/insertion into erythrocyte-like bilayers until the average hydrophobicity of the peptide core sequence is sufficiently high. Similarly, omwaprin's lack of haemolytic activity may be determined by its hydrophobicity status.

The antibacterial activity of cationic proteins is influenced by a combination of appropriate chain length, amino acid composition and positioning of apolar and positively charged residues, but the exact combination is still under study [43–45]. Structural constraints contributed by disulfide pairing are essential for many antibacterial proteins such as β-defensins [33], tachylepsins [46] and protegrins [47]. Reduced and alkylated omwaprin had no antibacterial activity, which suggests that the tertiary structure plays an important role in determining the function. Furthermore, deletion of the N-terminal charged 'tail' of omwaprin caused a loss of its antibacterial activity. According to our homology model, this positively charged N-terminal 'tail' is swung out of the disc-shaped backbone configuration.

There are several reports demonstrating antibacterial properties of snake venom components. One of the earliest reports was in 1968, where growth inhibition of *Staph. aureus* and *E. coli* by a basic low-molecular-mass direct lytic factor from *Hemachatus hemachatus* venom was demonstrated [48]. The haemolytic activity of the protein was also documented and it acts as a cationic detergent. Myotoxin II, a catalytically inactive Lys^{49} PLA_2 (phospholipase A_2) from the venom of *Bothrops asper*, shows antibacterial property towards Gram-positive and Gram-negative bacteria [49]. The C-terminal region of myotoxin II is essential for its activity, and its mechanism of action is by perturbing the bacterial membrane. Another myotoxic peptide, vgf-1, from *Naja naja atra* venom has antibacterial activity against drug-resistant *Mycobacterium tuberculosis in vitro* [50]. However, its functional domain is unknown. Several enzymes from snake venom also show antibacterial properties. For example, L-amino acid oxidase purified from the venom of *Crotalus adamanteus* has antibacterial activity against various Gram-negative bacteria [51]. However, they also possess various other biological functions, including action on platelets, induction of apoptosis, haemorrhagic effects and cytotoxicity. An L-amino acid oxidase (LAO1) from *Pseudechis australis* was 70 times more effective than tetracycline against *Aeromonas* [51]. The non-specific cytolytic effects of L-amino acid oxidase are due to production of H_2O_2. Recently, the antibacterial activity of myotoxins I (Lys^{49} PLA_2) and II (Asp^{49} PLA_2) isolated from *Bothrops jararacussu* venom against Gram-positive bacteria was reported [52]. The positively charged residues are essential for their activity. Electrostatic interactions between the PLA_2 molecules and bacterial membrane promote formation of negatively charged peptidoglycan pores in the bacterial cell membrane, allowing the penetration of PLA_2 into the bacteria [52]. Thus omwaprin is the first reported snake venom protein which specifically acts on bacteria without showing any haemolytic activity.

The biological significance of the presence of antibacterial proteins in the snake venoms is still unclear. Nevertheless, there are hypotheses suggesting that snake venom glands are evolutionarily related to salivary glands, which need to secrete antibacterial proteins [4]. Also, these antibacterial venom proteins, perhaps with other proteins of overlapping or similar functions, may help to inhibit bacterial growth in the swallowed prey [53]. The processes of ingestion and digestion are slow in many species of snakes. Hence antibacterial proteins in the venom might help to reduce the risk of putrefying before prey can be digested, or to protect the snake from bacterial pathogens in the ingested prey [53].

A number of low-molecular-mass antibacterial proteins have been isolated from bacteria, fungi, insects, plants and animals [54]. Cationic proteins, which vary widely in their amino acid composition, length and secondary structure, are widespread among them. These proteins possess a wide array of biological properties, such as antibacterial, antiviral, antifungal and anticancer activities [55]. The modes of antibacterial action of these proteins are by destabilizing the microbial membrane, inhibiting the synthesis of specific membrane proteins or stress proteins, interaction with DNA and arrest of DNA synthesis [54]. Considerable effort is being put into investigating the therapeutic potential of these proteins. The high degree of selectivity of the protein, its resistance to proteases tested and the potential to produce significant amounts of recombinant omwaprin make it an interesting candidate for such studies. Even though doses of omwaprin required for antibacterial activity are relatively high compared with those of some other antibacterial proteins, the activity can be improved by modifying the protein by substitution or deletion of residues without hindering the three-dimensional structure. Also, studies have to be performed to check whether the potency can be improved by synergy with conventional antibiotics or other antibacterial proteins [38].

In summary, we have isolated and functionally characterized omwaprin, a new member of the waprin family of snake venom proteins. Omwaprin shows selective antibacterial activity against Gram-positive bacteria. A homology model of the protein demonstrates the presence of a distinctly charged surface compared with that of the other antibacterial proteins. This may contribute to its selectivity. Further studies on the structure and the nature of interaction of omwaprin with the bacterial cell will provide new insights into its selective antibacterial activity. The established synthetic gene expression system will be useful for future studies.

This work was supported by Biomedical Research Council, Agency for Science and Technology, Singapore. We thank Dr Sanjay Swarup, Department of Biological Sciences, National University of Singapore (NUS), and Dr Tiow-Suan Sim, Department of Microbiology, NUS, for providing the bacterial strains. We also thank The Electron Microscopy Unit, Yong Loo Lin School of Medicine, NUS, for providing access to SEM facilities, and Dr Seetharama Jois, Department of Pharmacy, NUS, for help with homology modelling. D.G.N. was the recipient of a graduate research scholarship from NUS.

REFERENCES

1 Ferreira, S. H., Bartelt, D. C. and Greene, L. J. (1970) Isolation of bradykinin-potentiating peptides from *Bothrops jararaca* venom. Biochemistry **9**, 2583–2593
2 Marsh, N. A. (1998) Use of snake venom fractions in the coagulation laboratory. Blood Coagulation Fibrinolysis **9**, 395–404
3 Marsh, N. A. (2001) Diagnostic uses of snake venom. Haemostasis **31**, 211–217
4 de Lima, D. C., Alvarez, A. P., de Freitas, C. C., Santos, D. O., Borges, R. O., Dos Santos, T. C., Mendes, C. L., Rodrigues, C. R. and Castro, H. C. (2005) Snake venom: any clue for antibiotics and CAM? Evidence-Based Complement Altern. Med. **2**, 39–47
5 Sher, E., Giovannini, F., Boot, J. and Lang, B. (2000) Peptide neurotoxins, small-cell lung carcinoma and neurological paraneoplastic syndromes. Biochimie **82**, 927–936
6 Kordis, D. and Gubensek, F. (2000) Adaptive evolution of animal toxin multigene families. Gene **261**, 43–52
7 Bailey, G. S. (1998) Enzymes from Snake Venom, Alaken, Fort Collins
8 Kini, R. M. (1997) Venom Phospholipase A_2 Enzymes: Structure, Function and Mechanism, John Wiley and Sons, Chichester
9 Harvey, A. L. (1991) Snake Toxins, Pergamon Press, New York
10 Takasaki, C., Suzuki, J. and Tamiya, N. (1990) Purification and properties of several phospholipases A_2 from the venom of Australian king brown snake (*Pseudechis australis*). Toxicon **28**, 319–327
11 Braganca, B. M. and Sambray, Y. M. (1967) Multiple forms of cobra venom phospholipase A. Nature **216**, 1210–1211

12 Torres, A. M., Wong, H. Y., Desai, M., Moochhala, S., Kuchel, P. W. and Kini, R. M. (2003) Identification of a novel family of proteins in snake venoms: purification and structural characterization of nawaprin from *Naja nigricollis* snake venom. J. Biol. Chem. **278**, 40097–40104
13 Pung, Y. F., Kumar, S. V., Rajagopalan, N., Fry, B. G., Kumar, P. P. and Kini, R. M. (2006) Ohanin, a novel protein from king cobra venom: its cDNA and genomic organization. Gene **371**, 246–256
14 Araki, K., Kuroki, J., Ito, O., Kuwada, M. and Tachibana, S. (1989) Novel peptide inhibitor (SPAI) of Na^+,K^+-ATPase from porcine intestine. Biochem. Biophys. Res. Commun. **164**, 496–502
15 Thompson, R. C. and Ohlsson, K. (1986) Isolation, properties, and complete amino acid sequence of human secretory leukocyte proteinase inhibitor, a potent inhibitor of leukocyte elastase. Proc. Natl. Acad. Sci. U.S.A. **83**, 6692–6696
16 Wiedow, O., Schroder, J. M., Gregory, H., Young, J. A. and Christophers, E. (1990) Elafin: an elastase-specific inhibitor of human skin: purification, characterization, and complete amino acid sequence. J. Biol. Chem. **265**, 14791–14795
17 Larsen, M., Ressler, S. J., Lu, B., Gerdes, M. J., McBride, L., Dang, T. D. and Rowley, D. R. (1998) Molecular cloning and expression of ps20 growth inhibitor: a novel WAP-type "four-disulfide core" domain protein expressed in smooth muscle. J. Biol. Chem. **273**, 4574–4584
18 Hagiwara, K., Kikuchi, T., Endo, Y., Huqun, Usui K., Takahashi, M., Shibata, N., Kusakabe, T., Xin, H., Hoshi, S. et al. (2003) Mouse SWAM1 and SWAM2 are antibacterial proteins composed of a single whey acidic protein motif. J. Immunol. **170**, 1973–1979
19 Pung, Y. F., Wong, P. T., Kumar, P. P., Hodgson, W. C. and Kini, R. M. (2005) Ohanin, a novel protein from king cobra venom, induces hypolocomotion and hyperalgesia in mice. J. Biol. Chem. **280**, 13137–13147
20 Vila-Perello, M. and Andreu, D. (2005) Characterization and structural role of disulfide bonds in a highly knotted thionin from *Pyrularia pubera*. Biopolymers **80**, 697–707
21 Takemura, H., Kaku, M., Kohno, S., Hirakata, Y., Tanaka, H., Yoshida, R., Tomono, K., Koga, H., Wada, A., Hirayama, T. and Kamihira, S. (1996) Evaluation of susceptibility of Gram-positive and -negative bacteria to human defensins by using radial diffusion assay. Antimicrob. Agents Chemother. **40**, 2280–2284
22 Yenugu, S., Hamil, K. G., French, F. S. and Hall, S. H. (2004) The androgen-regulated epididymal sperm-binding protein, human β-defensin 118 (DEFB118) (formerly ESC42), is an antimicrobial β-defensin. Reprod. Biol. Endocrinol. **2**, 61
23 Ryadnov, M. G., Degtyareva, O. V., Kashparov, I. A. and Mitin, Y. V. (2002) A new synthetic all-D-peptide with high bacterial and low mammalian cytotoxicity. Peptides **23**, 1869–1871
24 Essigmann, B., Hespenheide, B. M., Kuhn, L. A. and Benning, C. (1999) Prediction of the active-site structure and NAD^+ binding in SQD1, a protein essential for sulfolipid biosynthesis in *Arabidopsis*. Arch. Biochem. Biophys. **369**, 30–41
25 Wu, J. and Watson, J. T. (1998) Optimization of the cleavage reaction for cyanylated cysteinyl proteins for efficient and simplified mass mapping. Anal. Biochem. **258**, 268–276
26 Wu, Z., Li, X., de Leeuw, E., Ericksen, B. and Lu, W. (2005) Why is the Arg^5–Glu^{13} salt bridge conserved in mammalian α-defensins? J. Biol. Chem. **280**, 43039–43047
27 Yenugu, S., Hamil, K. G., Birse, C. E., Ruben, S. M., French, F. S. and Hall, S. H. (2003) Antibacterial properties of the sperm-binding proteins and peptides human epididymis 2 (HE2) family: salt sensitivity, structural dependence and their interaction with outer and cytoplasmic membranes of *Escherichia coli*. Biochem. J. **372**, 473–483
28 Fry, B. G. (2005) From genome to "venome": molecular origin and evolution of the snake venom proteome inferred from phylogenetic analysis of toxin sequences and related body proteins. Genome Res. **15**, 403–420
29 Qi, J., Wu, J., Somkuti, G. A. and Watson, J. T. (2001) Determination of the disulfide structure of sillucin, a highly knotted, cysteine-rich peptide, by cyanylation/cleavage mass mapping. Biochemistry **40**, 4531–4538
30 Yenugu, S., Richardson, R. T., Sivashanmugam, P., Wang, Z., O'rand, M. G., French, F. S. and Hall, S. H. (2004) Antimicrobial activity of human EPPIN, an androgen-regulated, sperm-bound protein with a whey acidic protein motif. Biol. Reprod. **71**, 1484–1490
31 Couto, M. A., Harwig, S. S., Cullor, J. S., Hughes, J. P. and Lehrer, R. I. (1992) eNAP-2, a novel cysteine-rich bactericidal peptide from equine leukocytes. Infect. Immun. **60**, 5042–5047
32 Nagaoka, I., Hirota, S., Yomogida, S., Ohwada, A. and Hirata, M. (2000) Synergistic actions of antibacterial neutrophil defensins and cathelicidins. Inflamm. Res. **49**, 73–79
33 Yenugu, S., Hamil, K. G., Radhakrishnan, Y., French, F. S. and Hall, S. H. (2004) Antimicrobial actions of the human epididymis 2 (HE2) protein isoforms, HE2α, HE2β1 and HE2β2. Endocrinology **145**, 3165–3173
34 Nakajima, Y., Ishibashi, J., Yukuhiro, F., Asaoka, A., Taylor, D. and Yamakawa, M. (2003) Antibacterial activity and mechanism of action of tick defensin against Gram-positive bacteria. Biochim. Biophys. Acta **1624**, 125–130
35 Cociancich, S., Ghazi, A., Hetru, C., Hoffmann, J. A. and Letellier, L. (1993) Insect defensin, an inducible antibacterial peptide, forms voltage-dependent channels in *Micrococcus luteus*. J. Biol. Chem. **268**, 19239–19245
36 Gao, Y., van Belkum, M. J. and Stiles, M. E. (1999) The outer membrane of Gram-negative bacteria inhibits antibacterial activity of brochocin-C. Appl. Environ. Microbiol. **65**, 4329–4333
37 Devine, D. A. and Hancock, R. E. (2002) Cationic peptides: distribution and mechanisms of resistance. Curr. Pharm. Des. **8**, 703–714
38 Skerlavaj, B., Gennaro, R., Bagella, L., Merluzzi, L., Risso, A. and Zanetti, M. (1996) Biological characterization of two novel cathelicidin-derived peptides and identification of structural requirements for their antimicrobial and cell lytic activities. J. Biol. Chem. **271**, 28375–28381
39 Dempsey, C. E. (1990) The actions of melittin on membranes. Biochim. Biophys. Acta **1031**, 143–161
40 Johansson, J., Gudmundsson, G. H., Rottenberg, M. E., Berndt, K. D. and Agerberth, B. (1998) Conformation-dependent antibacterial activity of the naturally occurring human peptide LL-37. J. Biol. Chem. **273**, 3718–3724
41 Skerlavaj, B., Benincasa, M., Risso, A., Zanetti, M. and Gennaro, R. (1999) SMAP-29: a potent antibacterial and antifungal peptide from sheep leukocytes. FEBS Lett. **463**, 58–62
42 Glukhov, E., Stark, M., Burrows, L. L. and Deber, C. M. (2005) Basis for selectivity of cationic antimicrobial peptides for bacterial versus mammalian membranes. J. Biol. Chem. **280**, 33960–33967
43 Friedrich, C., Scott, M. G., Karunaratne, N., Yan, H. and Hancock, R. E. (1999) Salt-resistant α-helical cationic antimicrobial peptides. Antimicrob. Agents Chemother. **43**, 1542–1548
44 Kini, R. M. and Evans, H. J. (1989) A common cytolytic region in myotoxins, hemolysins, cardiotoxins and antibacterial peptides. Int. J. Pept. Protein Res. **34**, 277–286
45 Kini, R. M. and Evans, H. J. (1989) Role of cationic residues in cytolytic activity: modification of lysine residues in the cardiotoxin from *Naja nigricollis* venom and correlation between cytolytic and antiplatelet activity. Biochemistry **28**, 9209–9215
46 Matsuzaki, K., Nakayama, M., Fukui, M., Otaka, A., Funakoshi, S., Fujii, N., Bessho, K. and Miyajima, K. (1993) Role of disulfide linkages in tachyplesin–lipid interactions. Biochemistry **32**, 11704–11710
47 Mangoni, M. E., Aumelas, A., Charnet, P., Roumestand, C., Chiche, L., Despaux, E., Grassy, G., Calas, B. and Chavanieu, A. (1996) Change in membrane permeability induced by protegrin 1: implication of disulphide bridges for pore formation. FEBS Lett. **383**, 93–98
48 Aloof-Hirsch, S., de Vries, A. and Berger, A. (1968) The direct lytic factor of cobra venom: purification and chemical characterization. Biochim. Biophys. Acta **154**, 53–60
49 Paramo, L., Lomonte, B., Pizarro-Cerda, J., Bengoechea, J. A., Gorvel, J. P. and Moreno, E. (1998) Bactericidal activity of Lys^{49} and Asp^{49} myotoxic phospholipases A_2 from *Bothrops asper* snake venom – synthetic Lys^{49} myotoxin II-(115–129)-peptide identifies its bactericidal region. Eur. J. Biochem. **253**, 452–461
50 Xie, J. P., Yue, J., Xiong, Y. L., Wang, W. Y., Yu, S. Q. and Wang, H. H. (2003) *In vitro* activities of small peptides from snake venom against clinical isolates of drug-resistant *Mycobacterium tuberculosis*. Int. J. Antimicrob. Agents **22**, 172–174
51 Stiles, B. G., Sexton, F. W. and Weinstein, S. A. (1991) Antibacterial effects of different snake venoms: purification and characterization of antibacterial proteins from *Pseudechis australis* (Australian king brown or mulga snake) venom. Toxicon **29**, 1129–1141
52 Barbosa, P. S., Martins, A. M., Havt, A., Toyama, D. O., Evangelista, J. S., Ferreira, D. P., Joazeiro, P. P., Beriam, L. O., Toyama, M. H., Fonteles, M. C. and Monteiro, H. S. (2005) Renal and antibacterial effects induced by myotoxin I and II isolated from *Bothrops jararacussu* venom. Toxicon **46**, 376–386
53 Thomas, R. G. and Pough, F. H. (1979) The effect of rattlesnake venom on digestion of prey. Toxicon **17**, 221–228
54 De Smet, K. and Contreras, R. (2005) Human antimicrobial peptides: defensins, cathelicidins and histatins. Biotechnol. Lett. **27**, 1337–1347
55 Bals, R. (2000) Epithelial antimicrobial peptides in host defense against infection. Respir. Res. **1**, 141–150

Received 24 February 2006/11 October 2006; accepted 18 October 2006
Published as BJ Immediate Publication 18 October 2006, doi:10.1042/BJ20060318